1521-0111/89/4/407–412$25.00
MOLECULAR PHARMACOLOGY

http://dx.doi.org/10.1124/mol.115.101626
Mol Pharmacol 89:407–412, April 2016

Correlation between Activity and Domain Complementation in Adenylyl Cyclase Demonstrated with a Novel Fluorescence Resonance Energy Transfer Sensor[S]

Michael Ritt and Sivaraj Sivaramakrishnan

Department of Genetics, Cell Biology and Development, University of Minnesota, Minneapolis, Minnesota

Received September 3, 2015; accepted January 20, 2016

ABSTRACT

Adenylyl cyclase (AC) activity relies on multiple effectors acting through distinct binding sites. Crystal structures have revealed the location of these sites, and biochemical studies have explored the kinetics of ACs, but the interplay between conformation and activity remains incompletely understood. Here, we describe a novel fluorescence resonance energy transfer (FRET) sensor that functions both as a soluble cyclase and a reporter of complementation within the catalytic domain. We report a strong linear correlation between catalytic domain complementation and cyclase activity upon stimulation with forskolin and Gαs. Exploiting this, we dissect the mechanism of action of a series of forskolin analogs and a P-site inhibitor, 2′-d3′-AMP. Finally, we demonstrate that this sensor is functional in live cells, wherein it reports forskolin-stimulated activity of AC.

Introduction

Adenylyl cyclases (ACs) catalyze the production of cAMP from cellular ATP. Most ACs are integral membrane proteins with a membrane-tethered catalytic domain formed from a C1 and a C2 domain, which have a weak affinity for each other basally (>10 μM) and together have very little activity despite being held in close proximity (Tesmer and Sprang, 1998). These same domains, however, experience an ∼100-fold increase in affinity and a similar increase in activity when stimulated with effectors such as forskolin (FSK) and Gαs (Tesmer et al., 1997). Though all of these effectors enhance AC activity, they do so through distinct, spatially separated binding sites on the catalytic domain. Crystal structures of the catalytic domain show that the effectors bridge the C1 and C2 domains to varying extents (Tesmer et al., 1997). Hence, the degree to which complementation between C1 and C2 is a limiting step in effector-dependent activation of cyclase remains unclear and is the focus of this study.

Given that C1 and C2 are the minimal domains necessary for the catalytic activity of the cyclase, they have formed the focus of numerous studies examining the regulation of cyclase activity. Several versions of soluble ACs have been engineered by fusing the cytosolic domains (C1 and C2) of a single isoform (homodimer) or different isoforms (heterodimers) (Tang and Gilman, 1995; Dessauer and Gilman, 1996; Scholich et al., 1997). Although cyclase fusions have been used to gain insight into effector-dependent regulation of catalytic activity, they have not been leveraged to examine the conformation of the molecule. Here, we engineer a synthetic adenylyl cyclase conformation sensor (SYNAC) using an ER/K linker flanked by a fluorescence resonance energy transfer (FRET) pair within a cyclase fusion to generate.

The ER/K linker is a semirigid single protein alpha helix, consisting of a repeating sequence of glutamic acid (E) and arginine or lysine (R/K) residues, that separates the two domains beyond FRET range and provides a substantial barrier to nonspecific complementation (Sivaramakrishnan et al., 2008). Interactions between the domains flanking the ER/K linker bring the FRET pair into close proximity, leading to a measurable increase in FRET (Swanson and Sivaramakrishnan, 2014). In addition, effector-dependent complementation of the C1 and C2 domains stimulates cAMP generation, which can be measured using established assays.

Using these combined advantages, we observed a linear correlation between the affinity of the C1–C2 interaction and activity of the cyclase fusion. By exploiting this phenomenon, we demonstrate that a family of FSK-derived inhibitors known as deoxyforskolins (dFSK) is incapable of stimulating activity because of their inability to induce complementation. In contrast, although the P-site inhibitor 2′-d3′-AMP stabilizes the complemented conformation, it inhibits cyclase activity as it overlaps with the catalytic site. Finally, we find that the synergistic effects of Gαs and FSK on AC activity also translate to domain complementation, which can be observed in live cells.

This work was supported by the National Institutes of Health National Cancer Institute and National Institute of General Medical Sciences [Grants 1DP2 CA186752-01, 1-R01-GM-105646-01-A1]; and the American Heart Association Scientist Development Grant [Grant 13SDG14270009] (to S.S.).
dx.doi.org/10.1124/mol.115.101626.
[S] This article has supplemental material available at molpharm.aspetjournals.org.

ABBREVIATIONS: AC, adenylyl cyclase; BSA, bovine serum albumin; dFSK, deoxyforskolin; DMSO, dimethylsulfoxide; ER/K helix, glutamine arginine/lysine helix; FRET, fluorescence resonance energy transfer; FSK, forskolin; GTPγS, guanosine 5′-3-O-(thio)triphosphate; SYNAC, synthetic adenylyl cyclase; TEV, tobacco etch virus.

Materials and Methods

Constructs. Domains from AC II and V (*Homo sapiens*) were amplified via polymerase chain reaction from cDNAs acquired from the DNASU Plasmid Repository (Arizona State University, Tempe, AZ). SYNAC sensors were encoded as single polypeptide, from N- to C-terminus as ACII C2 (residues 822–1090) mCerulean TEV protease site 30 nm ER/K linker mCitrine ACV C1a (residues 444–670) mCitrine FLAG tag. One to two flexible Gly-Ser-Gly linkers connect all domains (see (Supplemental Fig. 1). The long splice variant of Gαs (*H. sapiens*) was amplified from cDNA (Open Biosystems, Huntsville, AL) and was cloned between unique restrictions sites with an N-terminal FLAG tag. β2AR-His-Gαs was generated by restriction enzyme cloning and consists of β2-AR followed by a 6xHis-tag followed immediately by a full-length Gαs, replicating the β2AR-His-Gαs fusion construct published by Seifert et al. (1998).

Insect Cell Culture and Protein Purification. Sf9 cells were cultured at 28°C in Sf900-II medium (Invitrogen) with 1% antibiotic-antimycotic (Invitrogen, Carlsbad, CA). Constructs were transiently transfected into Sf9 cells using Escort IV transfection reagent (Sigma-Aldrich, St. Louis, MO) in antibiotic-free medium. For FLAG-tag purification, cells were lysed 3 days after transfection in lysis buffer (0.5% IGEPAL, 4 mM $MgCl_2$, 200 mM NaCl, 7% sucrose, 20 mM HEPES (pH 7.5), 5 mM dithiothreitol, 50 μg/ml phenylmethylsulfonyl fluoride, 5 μg/ml aprotinin, 5 μg/ml leupeptin). Lysates were clarified by ultracentrifugation (200,000*g*, 4°C, 45 minutes) and bound to anti-FLAG M2 affinity gel (Sigma-Aldrich) at 4°C. The FLAG resin was washed with wash buffer (150 mM KCl, 20 mM HEPES [pH 7.5], 5 mM $MgCl_2$, 5 mM dithiothreitol, 50 μg/ml phenylmethylsulfonyl fluoride, 5 μg/ml aprotinin, 5 μg/ml leupeptin) and eluted overnight using FLAG peptide (Sigma-Aldrich). Gαs was further incubated overnight with either 115 μM GDP or guanosine 5′-3-*O*-(thio)triphosphate (GTPγS) (Sigma-Aldrich). SYNAC was desalted using Zeba Spin desalting columns (Pierce Biotechnology, Rockford, IL) into the assay buffer (50 mM HEPES [pH 8.0], 50 mM NaCl, 5 mM $MgCl_2$). Gαs was desalted into the same buffer containing 115 μM GDP or GTPγS.

Concentrations of SYNAC were determined by comparison of fluorescence intensity to known standards. Concentrations of Gαs were determined by gel electrophoresis and Coomassie staining compared with known concentration of bovine serum albumin (BSA). Protein integrity was assessed by gel electrophoresis, using fluorescent imaging (Typhoon gel imager; GE Healthcare Bio-Sciences, Pittsburgh, PA) and/or Coomassie staining. Additional integrity measurements were possible through the use of tobacco etch virus (TEV) protease. Briefly, protein samples were digested with TEV protease at room temperature for 2 hours, run on a 10% SDS-PAGE gel, and fluorescently scanned and/or Coomassie stained as described earlier to monitor protein fragment size as compared with intact and expected molecular weights.

Fluorometer Data Acquisition. Data were acquired on a FluoroMax-4 fluorometer (Horiba Scientific, Edison, NJ). FRET spectra were generated by exciting samples at 430 nm (spectral band pass 8 nm), and emission was scanned from 450–650 nm (band pass 4 nm). All data were taken at an estimated 30 nM SYNAC (based on mCerulean fluorescence; extinction coefficient: ~43,000 $M^{-1}cm^{-1}$).

Measurements were taken in assay buffer. All tubes were precoated with 0.05 mg/ml BSA for at least 5 minutes to limit nonspecific surface adsorption of proteins. This "precoat" solution was aspirated before addition of reaction components. For conditions containing FSK or dFSK analogs (Sigma-Aldrich), the equivalent controls were matched for concentration of dimethylsulfoxide (DMSO) (FSK stock 10 mM in 100% DMSO, dFSK analogs 5 mM in 100% DMSO). Gαs was used at a concentration of 800 nM.

All FRET ratios are represented as the average of three repeat measurements. For live cell fluorescence spectra, cultured Sf9 cells were harvested between 16 and 24 hours of expression. Cells were counted and resuspended to equal concentration (~2×10^6 cells/ml) in HEPES buffered saline (20 mM HEPES [pH 7.4], 5 mM KCl, 14.5 mM NaCl, 2 mM $CaCl_2$, 1 mM $MgCl_2$) with 0.2% dextrose and 1 mM ascorbic acid and measured as described earlier for fluorescence. Background subtraction was applied using nontransfected cells at the same concentration of cells per milliliter.

Cyclase Activity. The Kinase-Glo Max Assay (Promega, Madison, WI) was used to assess cyclase activity through ATP consumption. Briefly, the indicated conditions were pipetted into BSA-precoated tubes containing an estimated 30 nM SYNAC and 0.05 U inorganic pyrophosphatase (from *Escherichia coli;* New England Biolabs, Ipswich, MA). Either 500 μM or 1 mM ATP was added to initiate the reaction. Tubes were incubated at 30°C for 30 minutes before being divided into 20 μl aliquots and halted with an equal addition of Kinase-Glo Max reagent.

For experiments including inorganic pyrophosphate as a condition, samples were not pipetted with pyrophosphatase. Instead, the reaction was halted after 30 minutes by incubation at 65°C for 15 minutes. Samples were then quickly cooled to room temperature, and 0.05 units of pyrophosphatase were added; the samples were incubated at 30°C for 15 minutes and then processed as normal. ATP consumption was measured as luciferase activity as read by a 96-well microplate luminometer (M5e Spectramax spectrophotomter; Molecular Devices, Sunnyvale, CA).

cAMP Generation. The cAMP-Glo Assay (Promega) was used to assess cyclase activity in live cells. In live cells, Sf9 cells expressing equal amounts of protein were harvested 3 days after transfection, collected by centrifugation at 250*g* for 3 minutes, washed once with HEPES-buffered saline with dextrose (see earlier description), and resuspended at equal optical density. Cells were then treated for 10 minutes at room temperature with buffer, 100 μM isoproterenol (Sigma-Aldrich), or FSK, and processed according to the manufacturer's instructions. Luminescence was measured using a 96-well microplate luminometer (M5e Spectramax spectrophotometer; Molecular Devices).

Statistical Analysis. All activity data are the average of at least three independent repeats using different preparations of protein, and error is calculated as ± S.E.M. FRET data are the average of at least three spectra, and error is calculated as ± S.D. All nonspectra data were plotted and statistically analyzed in GraphPad Prism 6 (GraphPad Software, San Diego, CA). Spectra data are the average of three repeats and were plotted in Matlab (The Math Works, Natick, MA). Where presented and unless indicated otherwise, statistical significance is assessed using an unpaired Student's *t* test as performed by GraphPad Prism 6.

Results

The domains included in our construct are based on the work of Tesmer et al. (1997) and Hatley et al. (2002), and consist of C1a and C2a domains of ACII and ACV, respectively. This "catalytic core" of the C1a and C2a domains of ACs has been demonstrated to have a weak affinity between the two domains (~10 μM) and is sufficient to reconstitute cAMP generation (Tang and Gilman, 1995). In the SYNAC sensor, these domains are separated by a modular 30 nm ER/K linker that provides weak basal complementation (effective concentration ~100 nM) between the domains (Swanson and Sivaramakrishnan, 2014) as well as providing a substantial separation between the two sets of fluorophores used for the FRET readout (Fig. 1A). This allows both halves of the catalytic domain to be expressed at equal stoichiometry and with minimal basal activity but robust activation when stimulated with the specific AC-activating small molecule FSK (Fig. 1B). Two FRET acceptors (mCitrine) were used with a single FRET donor (mCerulean) as this greatly improved the dynamic range of the FRET sensor (data not shown).

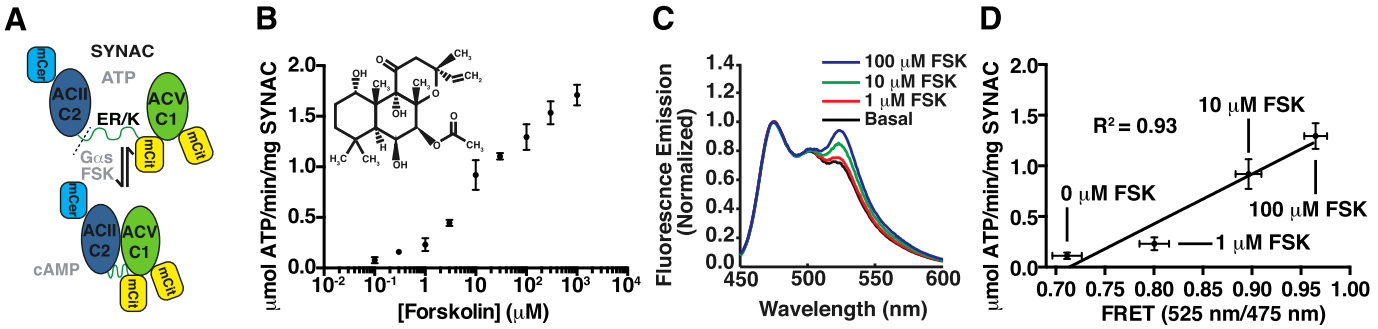

Fig. 1. Characterization of synthetic adenylyl cyclase (SYNAC). (A) Schematic diagram of SYNAC. Black dashed line indicates TEV protease cleavage site. Schematic shows the expected complementation of the ACII-C2 and ACV-C1 domains after stimulation with activated GαS (GTPγS) or FSK. (B) SYNAC displays FSK-stimulated activity in a concentration-dependent fashion. Activity is measured in terms of ATP metabolized by SYNAC. Inset is the structure of FSK. Data are mean ± S.E.M. of three independent repeats using three different preparations of protein. (C) FSK stimulates domain complementation in SYNAC. Normalized fluorescence emission spectrum (mCerulean, excitation 430 nm) of SYNAC stimulated with the indicated concentrations of FSK. Data are the average of three repeats. (D) FRET of SYNAC (mCit/mCer; 525 nm/475 nm) plotted against activity at the indicated concentrations of the compound. R^2 of 0.93 indicates a linear relationship between the two parameters. Activity data are mean ± S.E.M. of three independent repeats using three different preparations of protein. FRET data are mean ± S.D. of three spectra. Spectra are presented as mean without error bars for clarity.

FSK-driven activation of SYNAC is concentration dependent and remains fairly linear up to 300 μM FSK (Fig. 1B). The lack of saturation of SYNAC activity at high FSK concentrations is consistent with previous observations with cyclase fusions (Tang and Gilman, 1995). Given that there is a direct 1:1 correlation between cAMP production and ATP metabolism by ACs (Dessauer and Gilman, 1996), SYNAC activity can be easily monitored indirectly by ATP metabolism through a coupled luciferase assay. However, due to the production of pyrophosphate, a potent inhibitor of luciferase activity (Supplemental Fig. 2A) during the cyclization reaction, luminescence varies nonlinearly with residual ATP concentration. The addition of inorganic pyrophosphatase metabolizes pyrophosphate into phosphate, which does not interfere with luciferase activity. The incorporation of pyrophosphatase is sufficient to rectify this loss of luminescence and render a linear correlation between luminescence and residual ATP concentration (Supplemental Fig. 2B; see *Materials and Methods*).

FRET between the fluorophores mCerulean (mCer) and mCitrine (mCit) flanking the ER/K linker allows us to monitor the fraction of SYNAC in the closed conformation (Fig. 1C) (Sivaramakrishnan and Spudich, 2011). FRET response is directly proportional to activity, indicating that a closed conformation of SYNAC, wherein the two domains are in close proximity, has much greater activity than the open or low FRET conformation (Fig. 1D). This strongly supports the conclusions of Tesmer et al. (1997) drawn from the crystal structure of AC.

To further explore the relationship between conformation and activity, we investigated a number of FSK analogs that are known competitive inhibitors of ACs. These inhibitors, known as dFSK, lack an oxygen atom at various places on the diterpene rings of FSK and compete for the same binding site as FSK. Interestingly, when incubated with SYNAC, some of these dFSK compounds were still able to induce modest activity, albeit requiring much higher concentrations and to a far lower extent than FSK (Fig. 2, A–C). Further, when FRET was monitored, increasing concentrations of dFSK compounds corresponded with increased levels of FRET (Fig. 2D). Notably, the behavior of SYNAC in the presence of these dFSK compounds followed our observation of a linear correlation between activity and FRET (conformation) with FSK (Fig. 2E).

To test that these dFSK compounds were indeed capable of inhibiting FSK-stimulated activity, SYNAC was stimulated with 10 μM FSK under increasing concentrations of 1-dFSK (Fig. 2F). A reduction in the observed activity was visible at a high concentration of 1-dFSK and a similar drop in FRET was also observed (Supplemental Fig. 3). This suggests that 1-dFSK does bind SYNAC, albeit more weakly, and therefore is not as efficient at complementing the AC catalytic domain.

2′-d3′-AMP belongs to a class of uncompetitive inhibitors known as "P-site" inhibitors that have been shown to inhibit AC activity by occupying the ATP binding pocket along with pyrophosphate, prohibiting the enzyme from interacting with ATP (Dessauer and Gilman, 1997; Dessauer et al., 1999). Because of the low basal activity of SYNAC, SYNAC must first be stimulated to observe inhibition. Accordingly, SYNAC stimulated with FSK showed a significant decrease in activity when both 2′-d3′-AMP and pyrophosphate were present (Fig. 3A).

It must be noted that the 2′-d3′-AMP condition also contains residual pyrophosphate generated during cAMP synthesis, which can enhance 2′-d3′-AMP binding (see *Materials and Methods*). This likely contributes to the suppression of SYNAC activity with 2′-d3′-AMP alone. Counterintuitively, the domain complementation in SYNAC, as measured by FRET is further increased above the previous maxima of 100 μM FSK, in the presence of both pyrophosphate and 2′-d3′-AMP (stimulated with 100 μM FSK, Fig. 3B).

Our results suggest that a complemented state of the enzyme is being strongly stabilized by the presence of the inhibitor and pyrophosphate; hence its use in the crystal structure published by Tesmer et al. (1997). ATP also facilitates complementation (increase in FRET) but does not provide an increase above the stimulated maxima at 100 μM FSK, suggesting that the ATP-bound state is more transient in the FSK-stimulated conformation (Fig. 3B). The addition of pyrophosphate to the reaction by itself does not have a significant effect on either cyclase activity or FRET (Fig. 3, A and B).

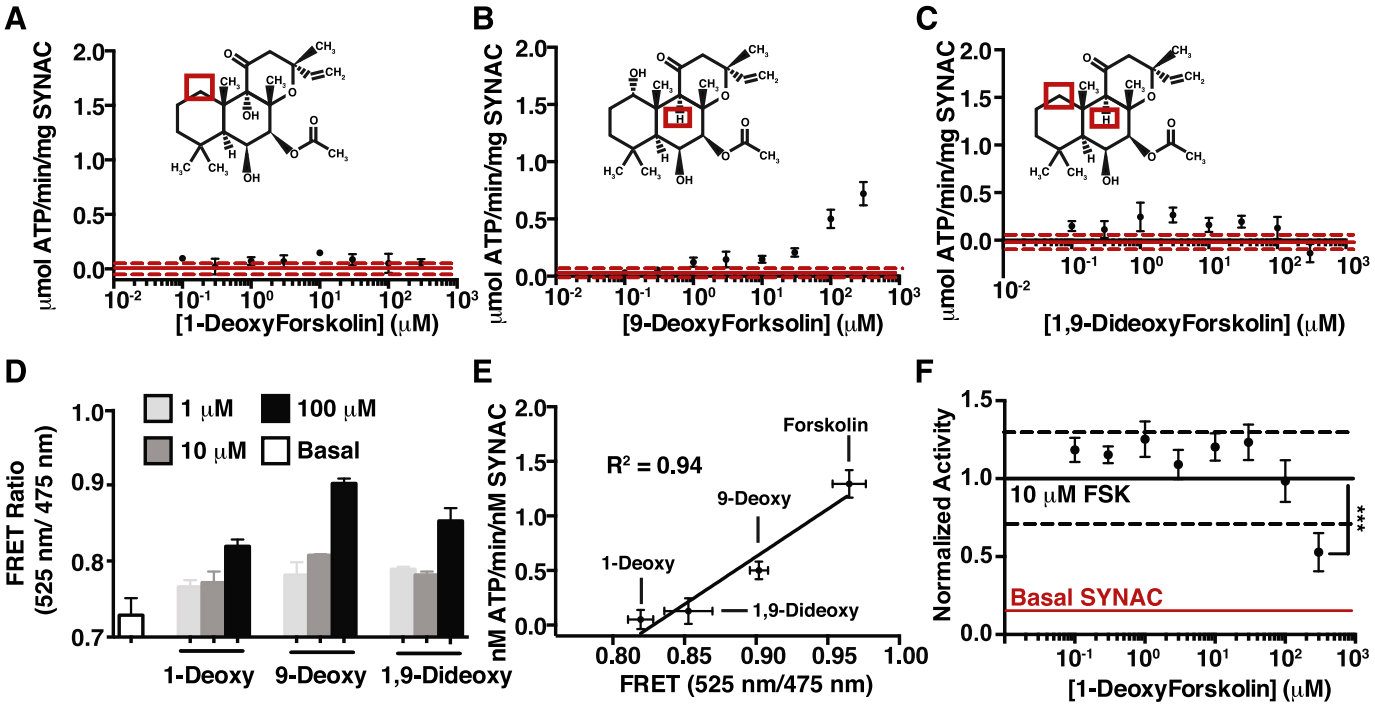

Fig. 2. Deoxyforskolin-stimulated complementation in SYNAC correlates with activity. (A–C) Effects of the indicated dFSK molecule on SYNAC activity. Insets represent structure of the indicated dFSK molecule with red boxes indicating differences from the structure of FSK. (D) Effects of the indicated dFSK molecules on SYNAC FRET at the indicated concentrations. (E) Activity of SYNAC plotted against FRET readout at 100 μM of the indicated compound. R^2 of 0.94 indicates a highly linear correlation. (F) Inhibition of 10 μM FSK-stimulated SYNAC activity by 1-day FSK at the indicated concentrations. The red line indicates basal activity levels for SYNAC. The solid black line indicates 10 μM FSK-stimulated SYNAC activity, with the dashed lines representing S.E.M. Data for this panel was normalized to FSK-stimulated activity, and significance was assessed by Student's *t* test (paired) to account for a systematic bias in data. Activity data are mean ± S.E.M. of three independent repeats using three different preparations of protein. FRET data are mean ± S.D. of three spectra. Significance assessed by Student's *t* test (unpaired) unless otherwise indicated. ***$P < 0.001$.

Besides FSK, the other canonical activator of ACs is the Gαs subunit. SYNAC displayed a synergistic increase in activity selectively with GTPγS-bound Gαs (Fig. 4A). Following previous trends in our data, this correlated with an increase in FRET for GTPγS-bound GαS incubated with SYNAC alone and a substantial increase in FRET when incubated with both FSK and GTPγS-bound Gαs (Fig. 4B). The synergistic effects of FSK treatment and GTPγS-bound Gαs were also visible when monitoring FRET (Fig. 4C). Notably, SYNAC reported a modest increase in FRET and activity when stimulated with GDP-bound Gαs, which has been reported as possessing a 10-fold lower affinity for cyclase (Sunahara et al., 1997).

Traditionally, insect (Sf9) cells have been used as a platform for probing G-protein-coupled receptor–G protein interactions and G protein–AC interactions due to the apparent lack of interference from endogenous G proteins (Schneider and

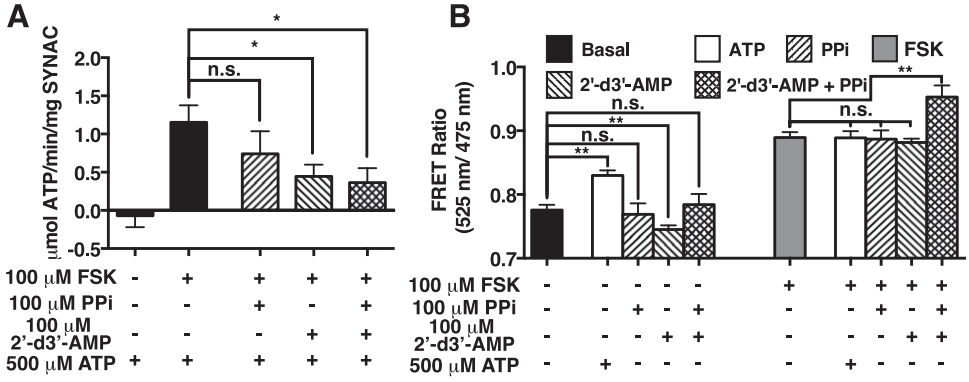

Fig. 3. 2′-d3′-AMP stimulates complementation in SYNAC without stimulating activity. (A) Effects of either 100 μM 2′-d3′-AMP, 100 μM pyrophosphate (PPi), or both together (as indicated) on SYNAC activity in the presence of 100 μM FSK. Pyrophosphate is being generated from FSK-stimulated SYNAC activity and inhibits cyclase activity in conjunction with 2′-d3′-AMP. In this assay, pyrophosphatase was added after the reaction had been stopped by denaturation at 65°C to remove pyrophosphate from solution, allowing detection by luciferase (see *Materials and Methods*). (B) The effects of 2′-d3′-AMP, ATP, and pyrophosphate on SYNAC FRET in the presence and absence of 100 μM FSK. Counterintuitively, the FRET detected in the presence of both 2′-d3′-AMP and pyrophosphate increases. Activity data are mean ± S.E.M. of three independent repeats using three different preparations of protein. FRET data are mean ± S.D. of three spectra. Significance assessed by Student's *t* test (unpaired). n.s. = not significant; *$P < 0.05$; **$P < 0.01$.

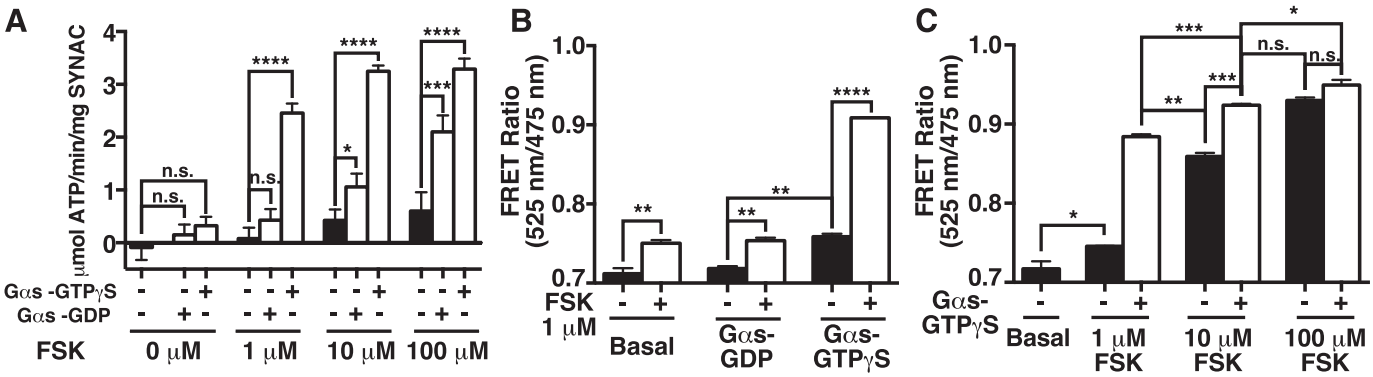

Fig. 4. Gαs stimulates SYNAC synergistically with FSK in a GTP-dependent manner. (A) FSK and Gαs synergistically stimulate SYNAC in a GTP-dependent manner. SYNAC was stimulated with 200 nM Gαs bound either to GDP or GTPγS at the indicated concentrations of FSK. (B) Complementation of SYNAC domains is enhanced by GTP-bound Gαs. FRET response of SYNAC stimulated with 200 nM Gαs bound either to GDP or GTPγS, with or without 1 μM FSK. (C) Complementation of SYNAC domains is synergistic to GTP-Gαs and FSK. FRET response of SYNAC with or without GTPγS bound Gαs (800 nM), in the presence of the indicated concentrations of FSK. Activity data are mean ± S.E.M. of three independent repeats using three different preparations of protein (both SYNAC and Gαs). FRET data are mean ± S.D. of three spectra. Significance assessed by Student's *t* test (unpaired). n.s. = not statistically significant; $^*P < 0.05$; $^{**}P < 0.01$; $^{***}P < 0.001$; $^{****}P < 0.0001$.

Seifert, 2010). When SYNAC was expressed in Sf9 cells and stimulated with FSK, we were able to observe AC activity above endogenous levels (Fig. 5A). SYNAC displayed enhanced basal cAMP production when cells were cotransfected with Gαs (Fig. 5B). Further, when SYNAC was coexpressed with a β2-AR-Gαs fusion protein (similar to that previously used by Seifert et al., 1998), we observed both basal and isoproterenol-stimulated cAMP production (Fig. 5C). Although, cAMP levels were detected to be much higher than basal levels when coexpressed with the β2-AR-Gαs, this is likely due to the increased activity of SYNAC basally in the presence of Gαs (Fig. 5b).

In spite of this increased basal activity, we are still able to see a statistically significant increase in signal from isoproterenol addition. However, inconsistent with the lack of any observable basal activity, SYNAC expressed alone in live cells had high basal FRET levels, but showed a significant increase in FRET ratio when stimulated with 100 μM FSK (Fig. 5D). Further, cells coexpressing SYNAC with Gαs or the β2-AR-Gαs fusion showed elevated basal levels of FRET as compared with SYNAC alone and β2-AR-Gαs showed a further increase over Gαs alone with SYNAC (Fig. 5D).

The elevated FRET levels are consistent with high basal cAMP generation in live cells. Isoproterenol stimulation leads to a small, but statistically significant increase above already high levels of cAMP (Fig. 5C). However, the corresponding FRET response was insignificant (Fig. 5D). This is unsurprising, considering the already high levels of FRET and the

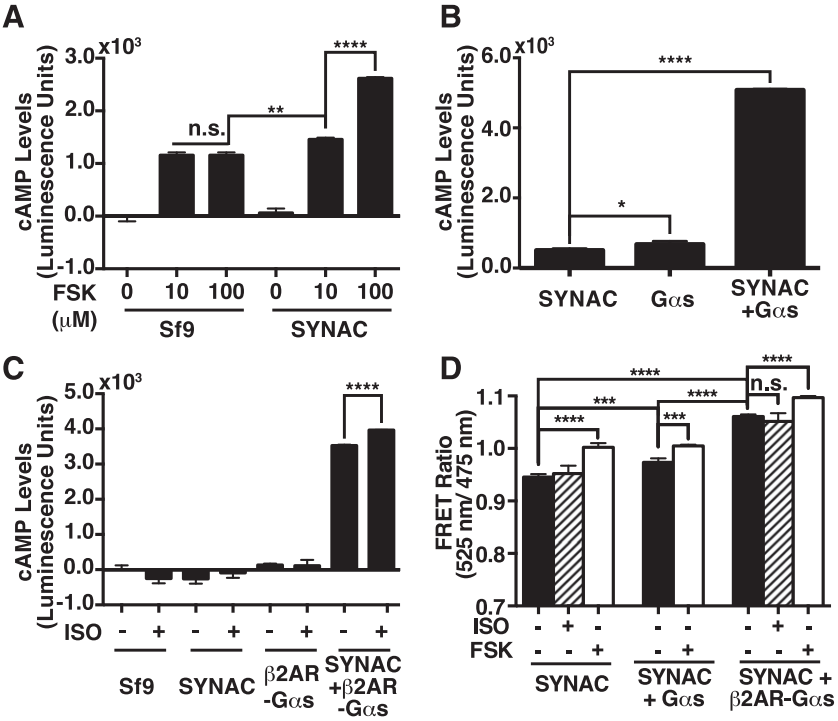

Fig. 5. Effector-stimulated activity of SYNAC in live cells. (A) cAMP generation in untransfected (Sf9) or SYNAC-expressing Sf9 cells (SYNAC) after treatment with indicated concentrations of FSK. cAMP levels are reported relative to untransfected, untreated cells. (B) Basal cAMP levels are elevated in Sf9 cells coexpressing SYNAC and Gαs, but not SYNAC or Gαs independently. (C) cAMP levels are basally elevated in cells coexpressing SYNAC and a β2-AR-Gαs fusion protein, and are further increased by addition of isoproterenol (ISO). cAMP levels in Sf9 cells expressing SYNAC, β2-AR-Gαs fusion, or coexpressing SYNAC and β2-AR-Gαs fusion with or without 100 μM isoproterenol treatment (10 minutes). (D) SYNAC FRET response in Sf9 cells after FSK (100 μM) and isoproterenol (100 μM) treatment with and without coexpression of Gαs and β2-AR-Gαs. Both conditions were incubated for 5 minutes with their respective conditions. Cells were held at equivalent optical density and expression as judged by mCerulean fluorescence. Activity data are mean ± S.E.M. of three independent repeats using three different preparations of protein. FRET data are mean ± S.D. of four spectra. Significance assessed by Student's *t* test (unpaired). n.s. = not significant; $^{**}P < 0.01$; $^{***}P < 0.001$; $^{****}P < 0.0001$.

incremental effect in cAMP generation. Overall, our sensor effectively recapitulates the activity state of cyclase in live cells.

Discussion

In this study a FRET-based biosensor, termed SYNAC, was used to demonstrate a linear correlation between catalytic domain complementation and enzymatic activity in AC. FRET-based biosensors have been used extensively to monitor AC activity in live cells. These A-kinase activity reporter sensors (Zhang et al., 2001) have been instrumental in mapping the spatiotemporal regulation of cAMP in response to a range of stimuli. However, they are designed to track cAMP generation rather than cyclase conformation. Also, although catalytic domain fusions of AC have previously been used to understand effector-dependent regulation of cyclase activity, they have not been engineered to probe the conformation of the molecule. The combination of using a cyclase fusion and a FRET-based detection system addresses the questions of cyclase conformation and enzymatic activity using a single construct.

SYNAC is capable of integrating information from activity and conformation. Using this advantage, our data suggest that even though the two catalytic domains are held in relative proximity to each other at the plasma membrane, the increase in affinity triggered by effector binding is necessary for cyclase activity. This correlation between affinity and activity also provides us with insight into the mechanisms of FSK and dFSK action. FSK binds cyclase relatively weakly in the absence of GαS as witnessed by a lack of saturation of both activity and catalytic domain complementation at concentrations approaching its solubility limit (Fig. 1B) (Tang and Gilman, 1995). The presence of GαS substantially increases the ability of FSK to complement and activate the cyclase (Fig. 4B).

dFSKs lack oxygens at C1 and/or C9 positions on the FSK diterpene ring, both of which are important elements of the FSK-binding interface (Tesmer et al., 1997). The absence of these oxygens disrupts catalytic domain complementation and, consequently, activity as well (Fig. 2, A–E). In addition, dFSKs bind SYNAC weakly, as reflected in the substantially higher concentrations required to inhibit FSK-stimulated SYNAC (Fig. 2F). Of note, however, is that the oxygen in the C1 position on the diterpene ring appears to be more important for activity than the oxygen in the C9 position, given the higher activity and complementation observed with 9-dFSK as compared with 1-dFSK (Fig. 2, A, B, and D).

Further, as illustrated by 2′-d3′-AMP, an increase in affinity is not always correlated with an increase in activity (Fig. 3, A and B). Instead, by occupying the active site, molecules such as 2′-d3′-AMP trap the cyclase in what would ordinarily appear to be an active conformation, based on complementation alone, but is actually catalytically silent. Hence, a two-pronged approach of monitoring both cyclase conformation and cAMP generation using SYNAC can provide additional information on the mechanism of drug action in ACs.

Cyclase activation stems from a combination of catalytic domain complementation and allosteric changes in the catalytic domain, which leads to a catalytically competent enzyme. SYNAC was engineered with a long structural ER/K linker flanked by a FRET pair to examine domain complementation in the context of enzymatic activity. Nonetheless, the inclusion of exogenous elements can alter interactions within the catalytic domain to influence the kinetics of this enzyme. Further, it is unclear to what extent the two halves of the catalytic domain are in proximity to each other in the native enzyme. Hence, it is possible that the catalytic domain is basally well-complemented in the full length molecule.

In this context, activation of the enzyme in response to effectors would stem primarily from subtle conformational changes that mirror the observed changes in domain complementation. Finally, the synthetic nature of the cyclase may influence its behavior in live cells. Contrary to the other findings reported in this work, there is an unexpectedly high level of FRET inside live cells in spite of a low level of basal activity (Fig. 5, A and D).

There are multiple factors that could contribute to this higher basal FRET, including clustering at the membrane, compartmentalization of the overexpressed protein, and interactions with other uncharacterized modulators of cyclase conformation. However, SYNAC does retain its sensitivity to effectors, and further studies are necessary to interpret measurements in live cells.

Authorship Contributions

Participated in research design: Ritt, Sivaramakrishnan.

Conducted experiments: Ritt.

Performed data analysis: Ritt, Sivaramakrishnan.

Wrote or contributed to the writing of the manuscript: Ritt, Sivaramakrishnan.

References

Dessauer CW and Gilman AG (1996) Purification and characterization of a soluble form of mammalian adenylyl cyclase. *J Biol Chem* **271**:16967–16974.

Dessauer CW and Gilman AG (1997) The catalytic mechanism of mammalian adenylyl cyclase. Equilibrium binding and kinetic analysis of P-site inhibition. *J Biol Chem* **272**:27787–27795.

Dessauer CW, Tesmer JJ, Sprang SR, and Gilman AG (1999) The interactions of adenylate cyclases with P-site inhibitors. *Trends Pharmacol Sci* **20**:205–210.

Hatley ME, Gilman AG, and Sunahara RK (2002) Expression, purification, and assay of cytosolic (catalytic) domains of membrane-bound mammalian adenylyl cyclases. *Methods Enzymol* **345**:127–140.

Schneider EH and Seifert R (2010) Sf9 cells: a versatile model system to investigate the pharmacological properties of G protein-coupled receptors. *Pharmacol Ther* **128**:387–418.

Scholich K, Barbier AJ, Mullenix JB, and Patel TB (1997) Characterization of soluble forms of nonchimeric type V adenylyl cyclases. *Proc Natl Acad Sci USA* **94**: 2915–2920.

Seifert R, Lee TW, Lam VT, and Kobilka BK (1998) Reconstitution of β2-adrenoceptor-GTP-binding-protein interaction in Sf9 cells–high coupling efficiency in a β2-adrenoceptor-G(s alpha) fusion protein. *Eur J Biochem* **255**:369–382.

Sivaramakrishnan S, Spink BJ, Sim AY, Doniach S, and Spudich JA (2008) Dynamic charge interactions create surprising rigidity in the ER/K alpha-helical protein motif. *Proc Natl Acad Sci USA* **105**:13356–13361.

Sivaramakrishnan S and Spudich JA (2011) Systematic control of protein interaction using a modular ER/K α-helix linker. *Proc Natl Acad Sci USA* **108**:20467–20472.

Sunahara RK, Dessauer CW, Whisnant RE, Kleuss C, and Gilman AG (1997) Interaction of Gsα with the cytosolic domains of mammalian adenylyl cyclase. *J Biol Chem* **272**:22265–22271.

Swanson CJ and Sivaramakrishnan S (2014) Harnessing the unique structural properties of isolated α-helices. *J Biol Chem* **289**:25460–25467.

Tang WJ and Gilman AG (1995) Construction of a soluble adenylyl cyclase activated by Gs alpha and forskolin. *Science* **268**:1769–1772.

Tesmer JJ and Sprang SR (1998) The structure, catalytic mechanism and regulation of adenylyl cyclase. *Curr Opin Struct Biol* **8**:713–719.

Tesmer JJ, Sunahara RK, Gilman AG, and Sprang SR (1997) Crystal structure of the catalytic domains of adenylyl cyclase in a complex with Gsα.GTPγS. *Science* **278**: 1907–1916.

Zhang J, Ma Y, Taylor SS, and Tsien RY (2001) Genetically encoded reporters of protein kinase A activity reveal impact of substrate tethering. *Proc Natl Acad Sci USA* **98**:14997–15002.

Address correspondence to: Dr. Sivaraj Sivaramakrishnan, 420 Washington Avenue SE, 4-130 MCB, Minneapolis, MN, 55455. E-mail: sivaraj@umn.edu

Correlation between activity and domain complementation in adenylyl cyclase demonstrated with a novel FRET sensor
Michael Ritt, Sivaraj Sivaramakrishnan
Molecular Pharmacology

Supplementary Figure 1- Sequence and domain organization of SYNAC

Amino Acid Sequence of SYNAC

MGTGMQNEYYCRLDFLWKNKFKKEREEIETMENLNRVLLENVLPAHVAEHFLARSLKN
EELYHQSYDCVCVMFASIPDFKEFYTESDVNKEGLECLRLLNEIIADFDDLLSKPKFSGVEK
IKTIGSTYMAATGLSAVPSQEHSQEPERQYMHIGTMVEFAFALVGKLDAINKHSFNDFKLR
VGINHGPVIAGVIGAQKPQYDIWGNTVNVASRMDSTGVLDKIQVTEETSLVLQTLGYTCTC
RGIINVKGKGDLKTYFVNTEMSRSLSQSNVASGSGTSGSGVSKGEELFTGVVPILVELDGDV
NGHKFSVSGEGEGDATYGKLTLKFICTTGKLPVPWPTLVTTLTWGVQCFARYPDHMKQH
DFFKSAMPEGYVQERTIFFKDDGNYKTRAEVKFEGDTLVNRIELKGIDFKEDGNILGHKLE
YNAISDNVYITADKQKNGIKANFKIRHNIEDGSVQLADHYQQNTPIGDGPVLLPDNHYLST
QSKLSKDPNEKRDHMVLLEFVTAAGITLGMDELYKEFGSGGSGENLYFQGGSGEEEEKKK
EEEEKKQKEEQERLAKEEAERKQKEEQERLAKEEAERKQKEEEERKQKEEEERKQKEEE
ERKLKEEQERKAAEEKKAKEEAERKAKEEQERKAEEERKKKEEEERLERERKEREEQEK
KAKEEAERIAKLEAEKKAEEERKAKEEEERKAKEEEERKKKEEQERLAKEKEEAERKAAE
EKKAKEEQERKEKEEAERKQRGSGGSGGAPVSKGEELFTGVVPILVELDGDVNGHKFSVS
GEGEGDATYGKLTLKFICTTGKLPVPWPTLVTTFGYGLMCFARYPDHMKQHDFFKSAMP
EGYVQERTIFFKDDGNYKTRAEVKFEGDTLVNRIELKGIDFKEDGNILGHKLEYNYNSHNV
YIMADKQKNGIKVNFKIRHNIEDGSVQLADHYQQNTPIGDGPVLLPDNHYLSYQSKLSKDP
NEKRDHMVLLEFVTAAGITLGMDELYKGSGGSGAPMEMKADINAKQEDMMFHKIYIQKH
DNVSILFADIEGFTSLASQCTAQELVMTLNELFARFDKLAAENHCLRIKILGDCYYCVSGLP
EARADHAHCCVEMGMDMIEAISLVREVTGVNVNMRVGIHSGRVHCGVLGLRKWQFDVW
SNDVTLANHMEAGGKAGRIHITKATLNYLNGDYEVEPGCGGERNAYLKEHSIETFLILRCT
QKRKEEKAMIAKMNRQRTNSIVDGSGGSGVSKGEELFTGVVPILVELDGDVNGHKFSVSG
EGEGDATYGKLTLKFICTTGKLPVPWPTLVTTFGYGLMCFARYPDHMKQHDFFKSAMPE
GYVQERTIFFKDDGNYKTRAEVKFEGDTLVNRIELKGIDFKEDGNILGHKLEYNYNSHNVY
IMADKQKNGIKVNFKIRHNIEDGSVQLADHYQQNTPIGDGPVLLPDNHYLSYQSKLSKDP
NEKRDHMVLLEFVTAAGITLGMDELYKGSGDYKDDDK*

Nucleotide Sequence of SYNAC

Methionine-Glycine
Atg gga

AgeI
aCCGGT

ACII-C2a (*H. sapiens*, aa 823-1083)
ATGCAGAATGAATATTACTGTAGGTTAGACTTCTTATGGAAGAACAAATTCAAAAAAGA
GCGGGAGGAGATAGAGACCATGGAGAACCTGAACCGCGTGCTGCTGGAGAACGTGCTTCC
CGCGCACGTGGCTGAGCACTTCCTGGCCAGGAGCCTGAAGAATGAGGAGCTATACCACCA
GTCCTATGACTGCGTCTGTGTCATGTTTGCCTCCATTCCGGATTTCAAAGAATTTTATAC
AGAATCCGACGTGAACAAGGAGGGCTTGGAATGCCTTCGGCTCCTGAACGAGATCATCGC
TGACTTTGATGATCTTCTTTCCAAGCCAAAATTCAGTGGAGTTGAAAAGATTAAGACCA
TTGGCAGCACATACATGGCAGCAACAGGTCTGAGCGCTGTGCCCAGCCAGGAGCACTCCC
AGGAGCCCGAGCGGCAGTACATGCACATTGGCACCATGGTGGAGTTTGCTTTTGCCCTGG
TAGGGAAGCTGGATGCCATCAACAAGCACTCCTTCAACGACTTCAAATTGCGAGTGGGTA
TTAACCATGGACCTGTGATAGCTGGTGTGATTGGAGCTCAGAAGCCACAATATGATATC
TGGGGCAACACTGTCAATGTGGCCAGTAGGATGGACAGCACCGGAGTCCTGGACAAAAT
ACAGGTTACCGAGGAGACGAGCCTCGTCCTGCAGACCCTCGGATACACGTGCACCTGTCG
AGGAATAATCAACGTGAAAGGAAAGGGGGACCTGAAGACGTACTTTGTAAACACAGAAA
TGTCAAGGTCCCTTTCCCAGAGCAACGTGGCATCC

Glycine-Serine-Glycine linker
GGAAGCGGA

SpeI
actagt

Gly-Ser-Gly linker
GGAAGCGGA

mCerulean
gtgagcaagggcgaggagctgttcaccggggtggtgcccatcctggtcgagctggacggcgacgtaaacggccacaag
ttcagcgtgtccggcgagggcgagggcgatgccacctacggcaagctgaccctgaagttcatctgcaccaccggcaagc
tgcccgtgccctggcccaccctcgtgaccaccctgacctggggcgtgcagtgcttcgcccgctaccccgaccacatgaag
cagcacgacttcttcaagtccgccatgcccgaaggctacgtccaggagcgcaccatcttcttcaaggacgacggcaacta
caagacccgcgccgaggtgaagttcgagggcgacaccctggtgaaccgcatcgagctgaagggcatcgacttcaagga
ggacggcaacatcctggggcacaagctggagtacaacgccatcagcgacaacgtctatatcaccgccgacaagcagaa
gaacggcatcaaggccaacttcaagatccgccacaacatcgaggacggcagcgtgcagctcgccgaccactaccagca
gaacacccccatcggcgacggccccgtgctgctgcccgacaaccactacctgagcacccagtccaagctgagcaaagac
cccaacgagaagcgcgatcacatggtcctgctggagttcgtgaccgccgccgggatcactctcggcatggacgagctgta
caAG

EcoRI
GAATTC

Gly-Ser-Gly x2
GGAAGCGGAGGAAGCGGA

TEV Protease site
GAAAACCTGTATTTTCAG

Gly-Gly-Ser-Gly linker
GGCGGAAGCGGA

ER/K linker (30 nm)
GAAGAGGAAGAGAAGAAGAAAGAAGAGGAAGAAAAGAAACAAAAAGAAGAACAAGAAA
GACTTGCAAAAGAAGAGGCAGAGAGAAAACAAAAAGAAGAACAAGAAAGACTTGCAAA
AGAAGAGGCAGAGAGAAAACAAAAGGAGGAAGAAGAGAGAAAACAAAAGGAAGAAGAA
GAGAGAAAACAAAAGGAGGAAGAAGAAAGAAAATTAAAGGAGGAACAAGAAAGAAAAG
CTGCAGAAGAAAAGAAAGCTAAAGAAGAAGCTGAGAGAAAGGCTAAAGAAGAACAAGA
AAGGAAAGCTGAAGAAGAGAGAAAGAAGAAAGAAGAGGAAGAAAGACTTGAAAGAGAA
AGAAAAGAGAGAGAAGAACAAGAAAAGAAAGCCAAAGAAGAGGCAGAGAGAATTGCAA
AGTTAGAGGCTGAAAAGAAGGCAGAAGAAGAAAGAAAAGCCAAAGAAGAAGAAGAGAG
AAAAGCCAAAGAAGAAGAGGAAAGAAAGAAGAAAGAGGAGCAAGAAAGACTTGCAAAA
GAAAAGGAAGAAGCAGAAAGAAAAGCTGCAGAGGAAAAGAAAGCTAAAGAAGAACAAG
AAAGAAAAGAAAAGGAAGAAGCAGAAAGAAAACAAAGA

Gly-Ser-Gly linker x2
GGCTCTGGCGGCTCTGGC

AscI Base added for frame shift
GGCGCGCC C

mCitrine
gtgagcaagggcgaggagctgttcaccggggtggtgcccatcctggtcgagctggacggcgacgtaaacggccacaag
ttcagcgtgtccggcgagggcgagggcgatgccacctacggcaagctgaccctgaagttcatctgcaccaccggcaagc
tgcccgtgccctggcccaccctcgtgaccaccttcggctacggcctgatgtgcttcgcccgctaccccgaccacatgaagc
agcacgacttcttcaagtccgccatgcccgaaggctacgtccaggagcgcaccatcttcttcaaggacgacggcaactac
aagacccgcgccgaggtgaagttcgagggcgacaccctggtgaaccgcatcgagctgaagggcatcgacttcaaggag
gacggcaacatcctggggcacaagctggagtacaactacaacagccacaacgtctatatcatggccgacaagcagaag
aacggcatcaaggtgaacttcaagatccgccacaacatcgaggacggcagcgtgcagctcgccgaccactaccagcag
aacaccccccatcggcgacggccccgtgctgctgcccgacaaccactacctgagctaccagtccaaactgagcaaagacc
ccaacgagaagcgcgatcacatggtcctgctggagttcgtgaccgccgccgggatcactctcggcatggacgagctgtac
aag

Gly-Ser-Gly linker x2
ggcagtggtggatca

AscI Base added for frame shift
ggCGCGCC C

ACV-C1a (*H. sapiens*, aa 442-667)
ATGGAGATGAAAGCAGACATCAACGCCAAGCAGGAGGATATGATGTTCCATAAGATTTA
CATCCAGAAACATGACAACGTGAGCATCCTGTTTGCTGACATCGAGGGCTTCACCAGCCT
GGCGTCCCAGTGCACTGCACAGGAACTGGTCATGACCCTCAACGAGCTCTTCGCCCGCTT
TGACAAGCTGGCCGCAGAGAATCACTGTTTACGTATTAAGATCCTTGGGGATTGTTATT
ACTGCGTCTCGGGGCTGCCTGAAGCAAGGGCTGACCACGCCCACTGCTGTGTGGAGATGG
GCATGGACATGATCGAGGCCATCTCGTTGGTCCGGGAGGTGACAGGGGTGAACGTGAAC
ATGCGTGTGGGAATTCACAGCGGGCGAGTACACTGCGGTGTCCTTGGTCTCAGGAAGTGG
CAGTTCGACGTCTGGTCTAACGATGTCACGCTAGCCAACCACATGGAGGCTGGCGGCAAG
GCAGGACGCATCCACATCACCAAGGCTACACTCAACTACCTGAATGGGGACTACGAGGTG
GAGCCAGGCTGTGGGGGCGAGCGCAACGCCTACCTCAAGGAGCACAGTATCGAGACCTTC
CTCATCCTGCGCTGCACCCAGAAGCGGAAAGAAGAGAAGGCCATGATCGCCAAGATGAAC
CGCCAGAGAACCAACTCCATC

SalI
GTCGAC

Gly-Ser-Gly linker x2
ggaagcggaGGCTCTGGC

mCitrine
gtgagcaagggcgaggagctgttcaccggggtggtgcccatcctggtcgagctggacggcgacgtaaacggccacaag
ttcagcgtgtccggcgagggcgagggcgatgccacctacggcaagctgaccctgaagttcatctgcaccaccggcaagc
tgcccgtgccctggcccaccctcgtgaccaccttcggctacggcctgatgtgcttcgcccgctaccccgaccacatgaagc
agcacgacttcttcaagtccgccatgcccgaaggctacgtccaggagcgcaccatcttcttcaaggacgacggcaactac
aagacccgcgccgaggtgaagttcgagggcgacaccctggtgaaccgcatcgagctgaagggcatcgacttcaaggag
gacggcaacatcctggggcacaagctggagtacaactacaacagccacaacgtctatatcatggccgacaagcagaag
aacggcatcaaggtgaacttcaagatccgccacaacatcgaggacggcagcgtgcagctcgccgaccactaccagcag
aacacccccatcggcgacggccccgtgctgctgcccgacaaccactacctgagctaccagtccaaactgagcaaagacc
ccaacgagaagcgcgatcacatggtcctgctggagttcgtgaccgccgccgggatcactctcggcatggacgagctgtac
aag

Gly-Ser-Gly linker
ggaagcgga

FLAG tag
GACTACAAGGACGATGACGACAAG

Stop NotI
TGA GCggccgc

Supplementary Figure 1- Sequence and domain organization of SYNAC

Amino acid and DNA sequences of SYNAC. Colors of domains correlate between the DNA sequence and the protein sequence. Briefly, the methionine and stop codons are uncolored, restriction sites used for cloning are colored red, the adenylyl cyclase II c2 domain is colored cyan, glycine-serine-glycine linkers are magenta, mCerulean is navy blue, the TEV site is colored grey, the ER/K linker is colored dark teal, mCitrine is yellow, adenylyl cyclase V c1 domain is colored green, and the FLAG tag is colored brown.

SUPPLEMENTAL FIGURE 2

Correlation between activity and domain complementation in adenylyl cyclase demonstrated with a novel FRET sensor

Ritt, Sivaramakrishnan

Molecular Pharmacology

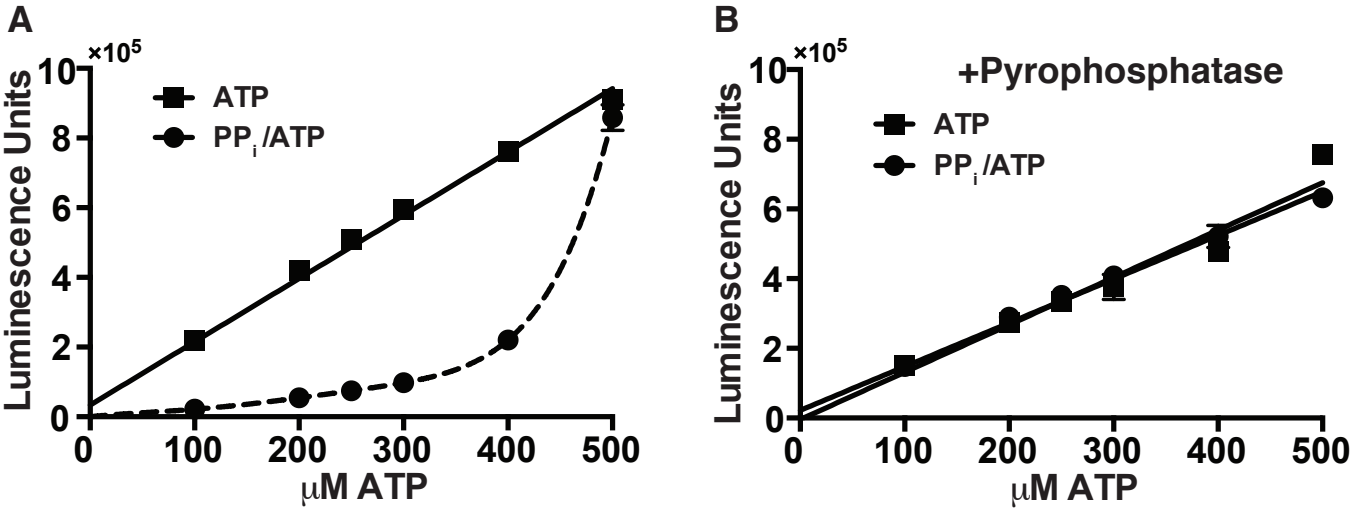

Supplementary Fig. 2. Luciferase inhibition by pyrophosphate.
(A) Pyrophosphate inhibits luciferase activity. Squares (solid line) show luminescence in terms of ATP concentration. Circles (dashed line) show luminescence in terms of ATP with a balance of pyrophosphate concentration up to 500 μM (300 μM ATP has 200 μM PPi; 100 μM ATP has 400 μM PPi, etc). This simulates ATP metabolism by cyclase (ATP is metabolized by cyclase into AMP and PPi). (B) The same reaction conditions in (a), but treated with pyrophosphatase in the reaction (see Methods). Data is representative

SUPPLEMENTARY FIGURE 3

Correlation between activity and domain complementation in adenylyl cyclase demonstrated with a novel FRET sensor

Ritt, Sivaramakrishnan
Molecular Pharmacology

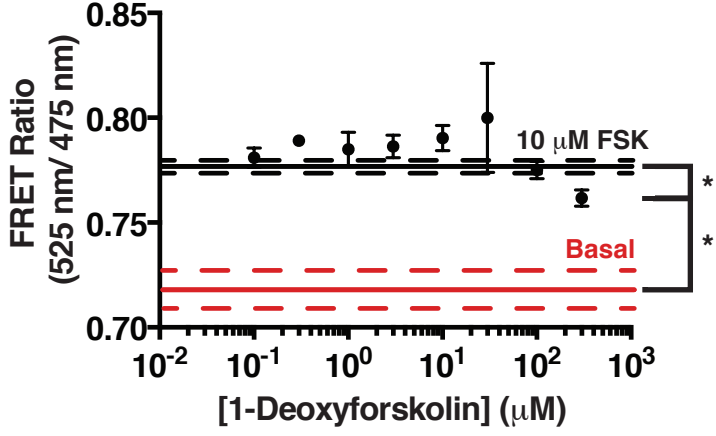

Supplementary Fig. 3. FRET readout of competitive inhibition of SYNAC by 1-deoxyforskolin.

FRET readout of SYNAC stimulated with 10 μM FSK in the presence of increasing concentrations of 1-deoxyforskolin. Red line is basal SYNAC activity and black line is 10 μM FSK stimulated SYNAC. The 300 μM deoxyforskolin point is significantly different from both basal and stimulated (Student's t-test, * = $p<0.05$). Dashed lines indicate error bars (+/- SEM) for their respective colored lines. Data is mean ± SEM of three in-dependent repeats